EPJ Web of Conferences **63**, 02008 (2013)
DOI: 10.1051/epjconf/ 20136302008

New dissipative non-Markovian model treatment of capture: the need for precise above-barrier cross sections

Maria Chushnyakova[a], Igor Gontchar

Physics and Chemistry Department, Omsk State Transport University, 644046 Omsk, Russia

Abstract. We performed quantitative theoretical analysis of the high precision data on the fusion excitation function in the reaction $^{16}\mathrm{O}+^{144}\mathrm{Sm}$ involving spherical nuclei. For this purpose the model is developed in which the collision process is described by the stochastic dynamical equations with the retarding friction and colored noise. The friction force is supposed to be proportional to the squared derivative of nucleus-nucleus interaction potential. The latter is calculated within the framework of the double folding approach with the density-dependent M3Y *NN*-forces. Varying the radial dissipation strength K_R and the matter diffuseness of $^{144}\mathrm{Sm}$ we reach χ^2 per point equal to 5.4. However the values of K_R and the friction retardation time τ_C appear to be strongly correlated. More high precision data are needed to make more definite conclusions about the values of K_R and τ_C.

In Ref. [1] the problem of the apparently large diffuseness of the Woods-Saxon nucleus-nucleus potential needed to fit a large number of precision capture excitation functions was formulated. We presume that the large diffuseness is an artifact masking some dynamical effects. In order to confirm or disprove this presumption we have developed a dynamical model and analyzed several precision capture excitation functions [2-4] for the reactions involving spherical nuclei. Qualitative results obtained within the framework of a simplified version of the model were published in Ref. [5].

Here we concentrate on the reaction $^{16}\mathrm{O}+^{144}\mathrm{Sm}$ and perform the χ^2 analysis of the precision excitation function measured in Ref. [3]. Note that both the problem of the large diffuseness and our dynamical model are relevant for the collision energy domain well above the average Coulomb barrier (only the cross sections $\sigma > 200$ mb must be considered). At the lower energies the fusion cross sections possess the structure which is described successfully by the coupled-channel approach [6].

Our model resembles the one of Refs. [7-9]: it is the dissipative trajectory model employing the surface friction. There are, however, several differences. First, the potential is very much different: we use the double folding potential based on the microscopically well founded M3Y *NN*-forces with the finite range exchange part and the density dependence [10]. By our knowledge, this potential was not used before in the dynamical models. Second, in our model, we account for the retarding friction and for the non-Markovian noise.

The nuclei involved in the reaction $^{16}\mathrm{O}+^{144}\mathrm{Sm}$ are spherical and rather stiff due to their closed shells. That is why we account only for two degrees of freedom corresponding to the radial and orbital motion. The dimensionless coordinates are $q = R/R_{PT}$ and φ being the angle between the line connecting the center of force with the fictitious particle at the given time moment and the linear momentum of the fictitious particle at $q >> 1$. Here R is the distance between the centers of the colliding nuclei and R_{PT} is equal to the sum of the half density radii: $R_{PT} = R_P + R_T$ (P and T denote the projectile and target nuclei, respectively).

The equations describing the collision process read

$$\frac{dp}{dt} = F_U + F_{cen} + \Phi_{Dq} + \xi\sqrt{2D_q}\,, \quad \frac{dq}{dt} = \frac{p}{m_q}\,, \quad \text{(1 a, b)}$$

$$F_U = -\frac{dU_{tot}}{dq}\,, \quad F_{cen} = \frac{\hbar^2 L^2}{m_q q^3}\,, \quad \text{(2 a, b)}$$

$$\Phi_{Dq} = \int_0^t F_{Dq}(s)\,\Gamma(t-s)\,ds\,, \quad \text{(3 a)}$$

[a] e-mail: maria.chushnyakova@gmail.com

$$F_{Dq}(t) = -\frac{p(t)}{m_q} K_R \left(\frac{dU_n[q(t)]}{dq} \right)^2, \qquad (3\text{ b})$$

$$\Gamma(t-s) = \frac{1}{\tau_C} \exp\left(-\frac{|t-s|}{\tau_C} \right), \qquad (4\text{ a})$$

$$D_q = \theta K_R \left(\frac{dU_n}{dq} \right)^2, \qquad (4\text{ b})$$

$$<\xi(t)>=0, \quad <\xi(t_1)\xi(t_2)>=\Gamma(t_1-t_2). \qquad (5\text{ a, b})$$

Here p stands for the linear momentum corresponding to the radial motion; F_U, F_{cen}, and Φ_{Dq} are the conservative, centrifugal, and retarding frictional forces, respectively. The latter is represented by the integral (3 a) due to the memory effects [11-13]. For the instant (local) radial frictional force F_{Dq} (see Eq. (3 b)) the surface friction expression [7, 8] is used. The memory kernel $\Gamma(t_1-t_2)$ (Eq. (4 a)) which also plays the role of the random force correlation function (Eq. (5 b)) is chosen following Refs. [11-13]. $U_{tot}(q)$ is the total interaction energy of two ions, it consists of the Coulomb $U_C(q)$ and nuclear $U_n(q)$ parts; $\hbar L$ is the projection of the orbital angular momentum onto the axis perpendicular to the reaction plane; $m_q = m_n A_P A_T \cdot R_{PT}^2 \left(A_P + A_T \right)^{-1}$ is the radial inertia parameter; m_n is the bare nucleon mass; K_R denotes the dissipation strength coefficient of the radial motion. The diffusion coefficient D_q, the temperature θ, and the friction coefficient $K_R \cdot (U_n')^2$ are related by the Einstein relation (4b). The memory effects are characterized by the correlation time τ_C which is expected to be of order of 0.1 zs [13].

According to our experience [5], the orbital motion is significantly slower than the radial motion. Therefore we choose the equations of the orbital motion to have the Markovian shape

$$\hbar \frac{dL}{dt} = F_{D\varphi} + b\sqrt{2D_\varphi}, \qquad \frac{d\varphi}{dt} = \frac{\hbar L}{m_q q^2}, \qquad (6\text{ a, b})$$

$$F_{D\varphi} = -\frac{\hbar(L-L_s)}{m_q} K_\varphi \left(\frac{dU_n}{dq} \right)^2, \qquad (7\text{ a})$$

$$D_\varphi = \theta K_\varphi \left(\frac{dU_n}{dq} \right)^2, \qquad (7\text{ b})$$

$$<b(t)>=0, \quad <b(t_1)b(t_2)>=\delta(t_1-t_2). \qquad (8\text{ a, b})$$

Here $F_{D\varphi}$ is the instant (local) dissipative force corresponding to the orbital motion; $L_s = 7L_0/5$ stands for the value of the orbital quantum number which L is relaxing to during its evolution (when L becomes equal to L_s the dinuclear system rotates as the solid body); K_φ denotes the orbital friction strength coefficient.

Accounting for only two degrees of freedom is clearly an approximation. Presently more elaborated time-dependent Hartree-Fock calculations of the heavy-ion collisions are available (see, e.g., Refs. [14-17]). In these works it was shown that the nucleon transfers [14] as well as the dynamical reagent deformation and neck formation [16, 17] might be of importance. However, the nucleon transfer is shown to be significant for the sub-barrier collision energies [14] whereas our model is relevant only for the above barrier collisions. According to our calculations [5], for the reactions $^{16}\mathrm{O} + {}^{92}\mathrm{Zr}$, $^{16}\mathrm{O} + {}^{144}\mathrm{Sm}$, and $^{16}\mathrm{O} + {}^{208}\mathrm{Pb}$ the capture is decided when $q > 1.25$ and the density in the overlap region is less than 25% of its central value (see, e.g. Figure 9 of Ref. [18]). For such reactions, the neck certainly appears and the reagents deform but after the capture is decided and therefore beyond the framework of our model.

In the present work we take the density dependence of the M3Y *NN* forces to have the following form [10]

$$F_{\mathrm{v}}(\rho_{FA}) = C_{\mathrm{v}} \left\{ 1 + \alpha_{\mathrm{v}} \exp\left(-\beta_{\mathrm{v}} \rho_{FA} \right) - \gamma_{\mathrm{v}} \rho_{FA} \right\} \qquad (9)$$

with $C_{\mathrm{v}} = 0.2728$, $\alpha_{\mathrm{v}} = 3.7367$, $\beta_{\mathrm{v}} = 1.8294$ fm^3, $\gamma_{\mathrm{v}} = 3.0$ fm^3.

In the M3Y double folding potential the nuclear matter density distribution is of crucial importance. The Woods-Saxon profile is used for this distribution:

$$\rho_A(r) = \rho_{0A} \left\{ 1 + \exp\left(\frac{r - R_A}{a_A} \right) \right\}^{-1}. \qquad (10)$$

Because ρ_{0A} is extracted from the normalization condition, the distribution is defined by the matter diffuseness a_A and the half density radius R_A (we take the proton and neutron densities having the same shape). The nuclear charge radius parameter R_q is equal to R_A whereas the matter diffuseness is related to the charge diffuseness a_q as follows:

$$a_A^2 = a_q^2 - \frac{5}{7\pi^2} \left(< r_{qp}^2 > - < r_{qn}^2 > \frac{N}{Z} \right) \qquad (11)$$

Here $< r_{qp}^2 >= 0.76$ fm^2 and $< r_{qn}^2 >= 0.11$ fm^2 [19]. In the first approximation over the small parameter $\pi^2 a_q^2 R_q^{-2}$, the charge radius and diffuseness are related with the root mean square charge radius R_{mq}

$$R_q = \sqrt{\frac{5}{3} \left(R_{mq}^2 - \frac{7\pi^2 a_q^2}{5} \right)}. \qquad (12)$$

We take the values of R_{mq} for both $^{16}\mathrm{O}$ and $^{144}\mathrm{Sm}$ from Ref. [20], whereas information about a_q is

available only for ^{16}O (see Ref. [21]). Therefore the value of the matter diffuseness for the target nucleus, a_{AT}, was taken to be an adjustable parameter. The second free parameter is K_R. Varying these two parameters we calculate the value χ^2 averaged over the number of points v, χ^2_v:

$$\chi^2_v = \frac{1}{v}\sum_{i=1}^{v}\left(\frac{\sigma_{itheor} - \sigma_{i\exp}}{\Delta\sigma_{i\exp}}\right)^2 . \qquad (13)$$

Here σ_{itheor} is the theoretical value of the cross section at the particular value of $E_{c.m.i}$, $\sigma_{i\exp}$ and $\Delta\sigma_{i\exp}$ are the experimental the cross section and its error at the same energy.

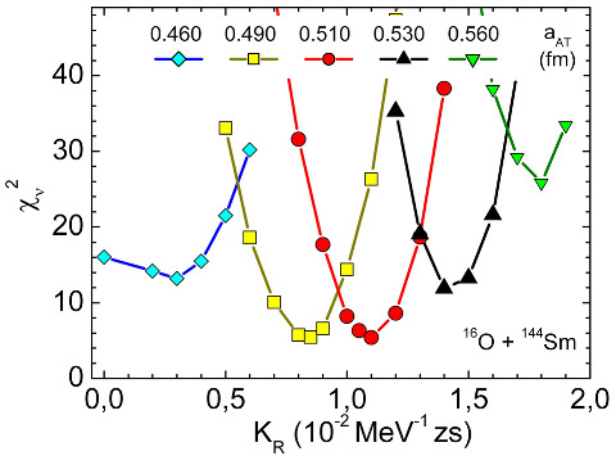

Figure 1. Results of the χ^2 analysis of the experimental fusion excitation function of Ref. [3]. τ_C =0.

The value of χ^2_v versus the radial friction strength coefficient is presented in Figure 1. Different curves correspond to the different values of a_{AT} as indicated in the figure. One sees the well pronounced minima of $\chi^2_v(K_R)$ for each value of the diffuseness. The best agreement with the data is achieved at $a_{AT} = (0.490 \div 0.510)$ fm and $K_R = (0.8 \div 1.1)\ 10^{-2}$ MeV^{-1} zs. This corresponds to $a_{qT} = (0.533 \div 0.552)$ fm which is in qualitative agreement with the values 0.522 fm for ^{154}Sm and 0.596 fm for ^{148}Sm from Ref. [21]. The values of the parameters providing the best agreement with the data are collected in Table 1.

It should be noted that the typical experimental error in [3] for the data points used in our analysis is 0.5%. We consider achieving, for such precision data, the quality of theoretical description corresponding to $\chi^2_v = 5.4$ to be a significant progress.

The calculations discussed above were performed for the instant friction and accordingly for the white noise ($\tau_C = 0$). The impact of the final correletaion time is illustrated by Figure 2. Here calculations are performed at $K_R = 4.0\ 10^{-2}$ MeV^{-1} zs. However increasing τ_C up to the value 0.4 zs brings the calculated cross sections in reasonable agreement with the data ($\chi^2_v = 7.5$).

Table 1. Parameters of matter and charge distribution providing the minimum value of $\chi^2_v = 5.4$. The value R_{mq} is taken from Ref. [20], a_q for ^{16}O is taken from Ref. [21], $R_q = R_A$ is calculated according to Eq. (12), a_A is calculated using Eq. (11).

Nucleus	R_{mq}, fm	R_q, fm	a_q, fm	a_A, fm
^{16}O	2.701	2.610	0.482	0.430
^{144}Sm	4.945	5.808	0.552	0.510
	4.945	5.848	0.533	0.490

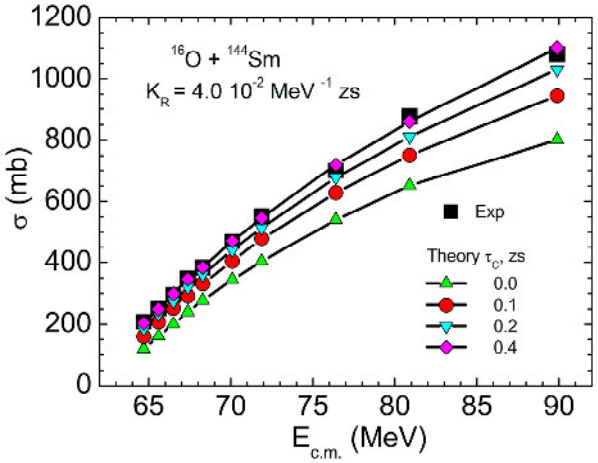

Figure 2. Experimental (scattered boxes, [3]) and calculated for different values of τ_C (symbols with lines) fusion excitation functions. $K_R = 4.0\ 10^{-2}$ MeV^{-1} zs, $a_{AT} = 0.510$ fm.

Similar monotonic behavior of the calculated excitation function approaching the experimental one is observed in Figure 3 for the case $\tau_C = 0$.

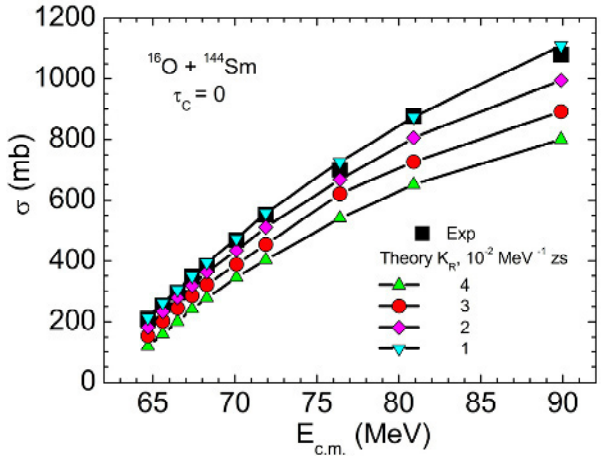

Figure 3. Experimental (scattered boxes, [3]) and calculated for different values of K_R (symbols with lines) fusion excitation functions. $\tau_C = 0$, $a_{AT} = 0.510$ fm.

Thus, the values of K_R and τ_C extracted from the fusion data seems to be not unique but rather correlated. The reason for this correlation is that, due to the

retardation the effective dissipation strength is always smaller than the instant one. Despite the correlation, the χ^2 analysis of the experimental above barrier precision fusion excitation function enables to place the lower limit on the instant dissipation strength K_R. Possibly such analysis, if been performed for reactions involving the same target nucleus ^{144}Sm but different spherical projectile nuclei like ^{28}Si, ^{40}Ca, ^{48}Ca, ^{58}Ni, would allow making more definite conclusions concerning the values of K_R and τ_C. Unfortunately, relevant data are absent in the literature.

Acknowledgments

M. V. C. is grateful to the Dmitry Zimin Foundation "Dynasty" and to the organizers of HIAS 2013 for financial support.

References

1. J.O. Newton, R.D. Butt, M. Dasgupta et al., Phys. Lett. B **586**, 219 (2004)
2. J.O. Newton, C.R. Morton, M. Dasgupta et al., Phys. Rev. C **64**, 064608 (2001)
3. J.R. Leigh, M. Dasgupta, D.J. Hinde et al., Phys. Rev. C **52**, 3151 (1995)
4. C.R. Morton, M. Dasgupta, D.J. Hinde et al., Phys. Rev. C **60**, 044608 (1999)
5. M.V. Chushnyakova and I.I. Gontchar, Phys. Rev. C **87**, 014614 (2013)
6. M. Dasgupta, D.J. Hinde, N. Rowley, A.M. Stefanini, Ann. Rev. Nucl. Part. Sci. **48**, 401 (1998)
7. D.H.E. Gross and H. Kalinowski, Phys. Rep. **45**, 175 (1978)
8. P. Fröbrich, B. Strack, M. Durand, Nucl. Phys. A **406**, 557 (1983)
9. P. Fröbrich, Phys. Rep. **116**, 337 (1984)
10. Dao T. Khoa, G.R. Satchler, W. von Oertzen, Phys. Rev. C **56**, 954 (1997)
11. D. Boilley, E. Suraud, Y. Abe, S. Ayik, Nucl. Phys. A **556**, 67 (1993)
12. Y. Abe, S. Ayik, P.-G. Reinhard, E. Suraud, Phys. Rep. **275**, 49 (1996)
13. A.E. Gegechkori, Yu.A. Anischenko et al, Phys. At. Nucl. **71**, 2007 (2008)
14. C. Simenel, Phys. Rev. Lett. **105**, 192701 (2010)
15. L. Guo and T. Nakatsukasa, EPJ Web of Conf. **38**, 09003 (2012)
16. A.S. Umar and V. E. Oberacker, Phys. Rev. C **73**, 054607 (2006)
17. C. Simenel, Eur. Phys. J. A **48**, 152 (2012)
18. I.I. Gontchar, M. Dasgupta, D.J. Hinde, J.O. Newton, Phys. Rev. C **69**, 024610 (2004)
19. G.R. Satchler and W.G. Love, Phys. Rep. **55**, 183 (1979)
20. I. Angeli, At. Dat. Nucl. Dat. Tables **87**, 185 (2004)
21. H. de Vries, C.W. de Jager, C. de Vries, At. Dat. Nucl. Dat. Tables **36**, 495 (1987)